Cell

Integrating Patterning Signals: Wnt/GSK3 Regulates the Duration of the BMP/Smad1 Signal

Luis C. Fuentealba,[1,2] Edward Eivers,[1,2] Atsushi Ikeda,[1,3] Cecilia Hurtado,[1] Hiroki Kuroda,[1,4] Edgar M. Pera,[1,5] and Edward M. De Robertis[1,*]

[1]Howard Hughes Medical Institute and Department of Biological Chemistry, University of California, Los Angeles, CA 90095-1662, USA

[2]These authors contributed equally to this work.

[3]Present address: Kyoto University Graduate School of Pharmaceutical Sciences, Kyoto 606-8501, Japan.

[4]Present address: Faculty of Education (Sciences), Shizuoka University, 836 Ohya, Suruga-ku, Shizuoka-city 422-8529, Japan.

[5]Present address: Lund Stem Cell Center, BMC, B13, Klinikgatan 26, S-22184 Lund, Sweden.

*Correspondence: ederobertis@mednet.ucla.edu

DOI 10.1016/j.cell.2007.09.027

SUMMARY

BMP receptors determine the intensity of BMP signals via Smad1 C-terminal phosphorylations. Here we show that a finely controlled cell biological pathway terminates this activity. The duration of the activated pSmad1^{Cter} signal was regulated by sequential Smad1 linker region phosphorylations at conserved MAPK and GSK3 sites required for its polyubiquitinylation and transport to the centrosome. Proteasomal degradation of activated Smad1 and total polyubiquitinated proteins took place in the centrosome. Inhibitors of the Erk, p38, and JNK MAPKs, as well as GSK3 inhibitors, prolonged the duration of a pulse of BMP7. Wnt signaling decreased pSmad1^{GSK3} antigen levels and redistributed it from the centrosome to cytoplasmic LRP6 signalosomes. In *Xenopus* embryos, it was found that Wnts induce epidermis and that this required an active BMP-Smad pathway. Epistatic experiments suggested that the dorsoventral (BMP) and anteroposterior (Wnt/GSK3) patterning gradients are integrated at the level of Smad1 phosphorylations during embryonic pattern formation.

INTRODUCTION

Understanding how cells integrate multiple signaling pathways to achieve specific cell differentiations is one of the major challenges in cell and developmental biology. Embryonic patterning in *Xenopus* is regulated by gradients of growth factors and their antagonists, with bone morphogenetic proteins (BMPs) controlling dorsal-ventral (D-V) and Wnt signals anterior-posterior (A-P) cell fates (Niehrs, 2004). This positional information must be seamlessly integrated, for when a blastula is cut in half, the embryo can self-regulate, forming perfect identical twins (De Robertis, 2006). In the ectoderm, the main cell differentiation decision is between neural and epidermal tissues, for which excellent molecular markers exist. Neural tissue differentiates when BMP signaling is inhibited by BMP antagonists or depletion by anti-BMP morpholino (MO) oligos, whereas epidermis is formed at high BMP signaling levels (Harland, 2000; Reversade and De Robertis, 2005). BMP receptors (BMPR) are serine/threonine protein kinases that signal by phosphorylating the transcription factors Smad1/5/8 at C-terminal sites (SS[PO_3]VS[PO_3]), causing their activation and nuclear translocation (Shi and Massagué, 2003; Feng and Derynck, 2005).

Neural tissue can also be induced by receptor tyrosine kinases (RTKs) such as FGF and IGF receptors via the activation of mitogen-activated protein kinase (MAPK) (reviewed in Wilson and Edlund, 2001; De Robertis and Kuroda, 2004; Stern, 2005). This neural-inducing activity can be explained in part by an inhibitory phosphorylation in the linker (middle) region of Smad1 at four conserved MAPK (PXS[PO_3]P) sites (Pera et al., 2003; Kuroda et al., 2005). This linker region MAPK phosphorylation was first discovered in cultured cells treated with EGF (Kretzschmar et al., 1997) and recently reported to promote polyubiquitinylation of Smad1 by the Smurf1 E3-ubiquitin ligase (Zhu et al., 1999; Sapkota et al., 2007), a finding independently confirmed here. FGF/MAPK signals are known to oppose BMP/Smad1 in many developing organs (De Robertis and Kuroda, 2004). Remarkably, mouse phosphorylation-resistant mutations in the MAPK sites of Smad1, introduced by homologous knock-in, generated embryonic fibroblasts in which the transcriptional activation of a reporter gene by BMP becomes resistant to repression by addition of FGF (Aubin et al., 2004; Sapkota et al., 2007). Thus, the role of Smad1 as an interface for integrating RTK and BMP signals is firmly established.

Although less generally recognized, the Wnt signaling pathway also influences neural induction. Wnts play multiple roles during development: at the early blastula stage, canonical Wnt signaling provides a dorsalizing signal via activation of xTcf3 (Harland, 2000; Heasman, 2006), and at the neurula stage, it regulates neuronal differentiation via inhibition of NeuroD (Marcus et al., 1998). At the gastrula stage, overexpression of Wnt8 causes antineural effects in *Xenopus* (Christian and Moon, 1993). Wnt antagonists such as Dickkopf-1 (Dkk1) and secreted Frizzled-related proteins (sFRPs), promote neural differentiation in *Xenopus*, chick, and mouse ES cells (Glinka et al., 1998; Wilson and Edlund, 2001; Aubert et al., 2002). The canonical Wnt pathway signals through the inhibition of glycogen synthase kinase 3 activity (Logan and Nusse, 2004). GSK3 is a protein kinase that usually requires prephosphorylated substrates, phosphorylating Ser/Thr residues located four amino acids upstream of sites primed by other kinases (Cohen and Frame, 2001). Frequently, as in the case of β-catenin, such coupled phosphorylations by two protein kinases are followed by polyubiquitination and degradation in the proteasome (Liu et al., 2002; Cohen and Frame, 2001). This project was initiated when we noticed conserved GSK3 sites in vertebrate Smad1/5/8 proteins that could be phosphorylated by GSK3 after priming by MAPK. This was exciting, because a pathway in which

$$\text{Dkk} \dashv \text{Wnt} \dashv \text{GSK3} \dashv \text{pSmad1}^{\text{Cter}} \dashv \text{Neural plate}$$

could potentially explain the proneural effects of anti-Wnts.

In the present study, we demonstrate that phosphorylation at the GSK3 sites represses the transcriptional activity of Smad1 by enhancing proteasomal degradation of $\text{pSmad1}^{\text{Cter}}$. We found that GSK3 phosphorylation is an essential requirement for polyubiquitination. Pulse-chase experiments with BMP7 revealed a novel cellular pathway that regulates the duration of the BMP signal. First, BMPR causes C-terminal phosphorylation ($\text{pSmad1}^{\text{Cter}}$) and nuclear translocation. Next, the $\text{pSmad1}^{\text{MAPK}}$ phosphorylation is mediated by MAPK enzymes (Erk, p38, and JNK) in the nucleus. Subsequently, GSK3 recognizes the prephosphorylated linker region, generating $\text{pSmad1}^{\text{GSK3}}$ at an unknown cellular location. The triply phosphorylated protein is transported along microtubule-like structures to the centrosome. The centrosome is the cellular location at which proteasomes normally accumulate in many cell types (Badano et al., 2005). The GSK3 activity that phosphorylates Smad1 was regulated by Wnt3a protein addition in cultured cells, leading to the accumulation of $\text{pSmad1}^{\text{Cter}}$. A constitutively active low-density lipoprotein receptor-related protein 6 (CA-LRP6) caused redistribution of $\text{pSmad1}^{\text{GSK3}}$ from the centrosome to cytoplasmic particles resembling the recently described LRP6 signalosomes (Bilic et al., 2007). In vivo epistatic experiments indicated that Smad1 phosphorylations by GSK3 play a key role in mediating the effects of Wnt signaling on neural development at the gastrula stage. In dissociated ectodermal cells, overexpression of Wnt8 and its coreceptor LRP6 induced epidermal differentiation in a Smad1/5/8-dependent manner. The results suggest that a branch of the canonical Wnt pathway signals through the stabilization of BMP-Smad signals.

RESULTS

GSK3 Phosphorylation Inhibits Smad1 Function

Inspection of the Smad1 sequence revealed four GSK3 sites located four amino acids upstream of the PXSP Erk/MAPK sites in the linker region (Figure 1A). These potential GSK3 sites were conserved in BMP-responsive Smad1/5/8 across vertebrates and in *Drosophila* Mad (Figure S1 in the Supplemental Data available online). Phosphorylation-resistant mutations (Ser/Thr to Ala) were introduced into a human Smad1 expression construct (Kretzschmar et al., 1997) previously characterized in *Xenopus* embryos (Pera et al., 2003; Kuroda et al., 2005). These sites were mutated individually or in combination; strongest effects were found when all four GSK3 sites were mutated (data not shown) in a construct designated SGM (Figure 1B). The phenotypic effects of SGM were compared to those of Smad1 wild-type (SWT) and Smad1 mutated at the MAPK sites (designated SMM). Overexpression of mRNA encoding GSK3 or MAPK phosphorylation-resistant mutants in early *Xenopus* embryos resulted in hyperactive Smad1 proteins that caused strongly ventralized phenotypes, as indicated by transcript accumulation of the BMP-inducible marker *Sizzled* (Figures 1C–1F). A constitutively active phospho-mimetic form of Smad1, in which the C-terminal SVS phosphorylation sites were mutated into EVE (designated SEVE; Figure 1G), provided a novel reagent independent of BMPR signaling (compare Figure 1D to Figure 1H). GSK3 and MAPK phosphorylation-resistant mutants of SEVE strongly induced *Sizzled*, not only ventrally but also ectopically in the floor plate (Figures 1I and 1J, insets). We conclude that the function of the putative GSK3 phosphorylations in vivo, like those of MAPK, is to downregulate Smad1 activity.

We next tested whether Smad1 was a substrate for GSK3 that required priming by MAPK (Cohen and Frame, 2001). The entire linker region of human Smad1 was tagged with six histidines, expressed in *E. coli*, and purified. In vitro phosphorylations were performed in two stages, and it was found that GSK3β caused the incorporation of [γ-^{32}P]ATP by Smad1 linker protein, but only after prephosphorylation by Erk/MAPK (Figure 1K, compare lanes 2 and 4).

Antibody reagents specific for human phospho-$\text{Smad1}^{\text{GSK3}}$ (p-Serine 210) and phospho-$\text{Smad1}^{\text{MAPK}}$ (p-Serine 214) were developed. A synthetic peptide (SS[PO_3]DPGS[PO_3]PFQMPADT) proved extremely antigenic. After affinity purification on a column of the same peptide phosphorylated only in Ser214, one rabbit produced a very high titer antibody for $\text{pSmad1}^{\text{MAPK}}$, such

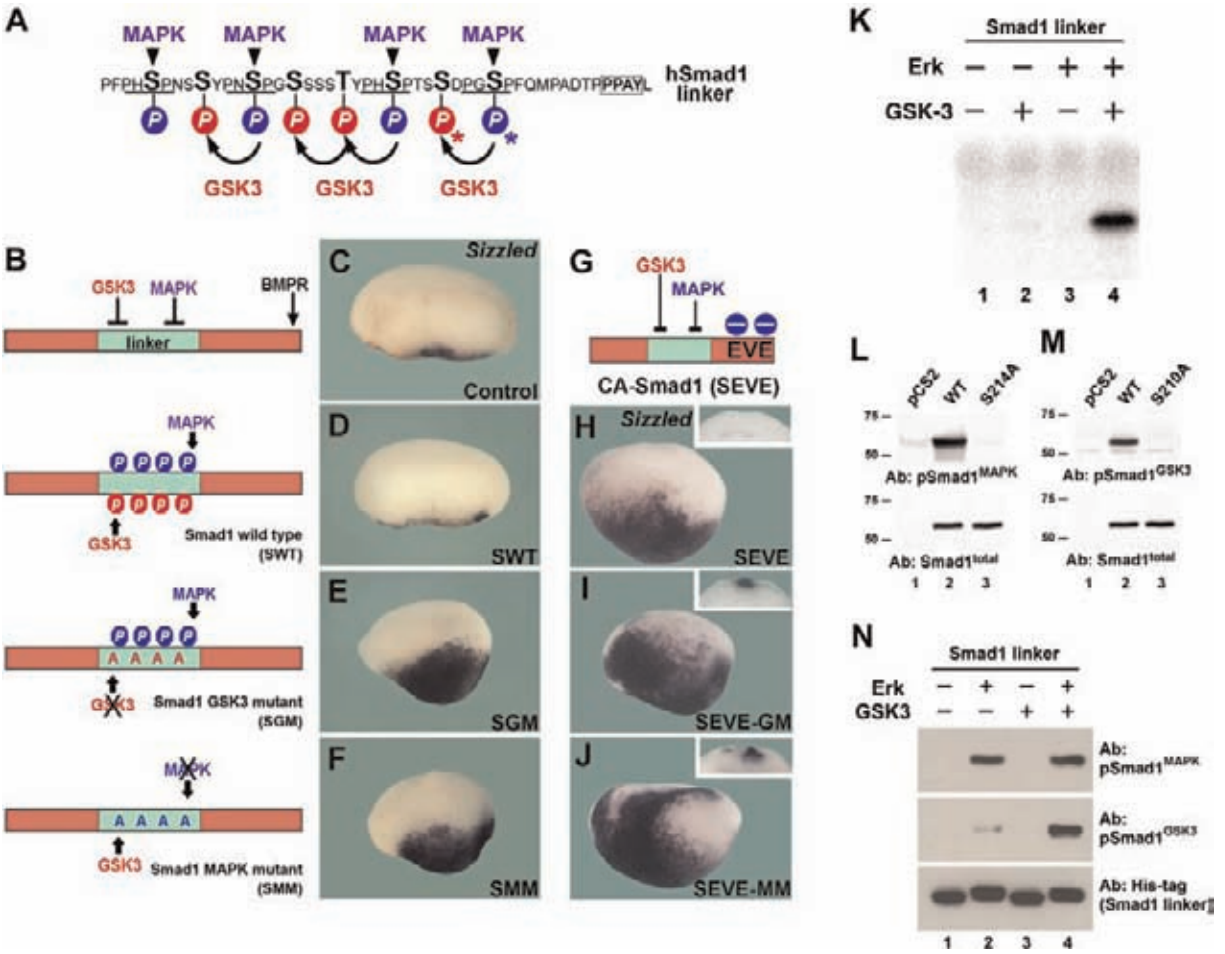

Figure 1. Smad1 Is Phosphorylated and Inhibited by GSK3

(A) Smad1 contains MAPK (blue) and GSK3 (red) phosphorylation sites in its linker region. The PPAY binding site of Smurf1 is boxed and serines 210 and 214 used to raise antibodies indicated by asterisks.

(B) Smad1 constructs encoding Smad1 wild-type (SWT) or phosphorylation-resistant mutants for GSK3 (SGM) and MAPK (SMM) sites.

(C–F) Injection of *SGM* or *SMM*, but not of *SWT*, mRNA increased expression of the ventral marker *sizzled* in *Xenopus* embryos.

(G) A BMP-independent phospho-mimetic activated Smad1 (SEVE) in which the SVS terminus was mutated into EVE.

(H–J) Activity of SEVE is increased by phosphorylation-resistant linker mutations.

(K) GSK3 radioactively phosphorylates Smad1 in vitro, but only when primed by MAPK. The recombinant Smad1 linker substrate was about 90% pure in polyacrylamide gels (data not shown).

(L and M) Phospho-specific antibodies for hSmad1 Ser214 (pSmad1^{MAPK}) and Ser210 (pSmad1^{GSK3} antibody B was used).

(N) Phospho-specific antibodies (pSmad1^{MAPK} and pSmad1^{GSK3}-A) demonstrate that GSK3 phosphorylation of recombinant Smad1 requires MAPK priming, in nonradioactive Western blots. Recombinant Smad1 substrate was used in the same amount as in (K).

that it detected overexpressed hSmad1-wt, but not the phosphorylation-resistant mutant S214A, at dilutions of 1:200,000 (Figure 1L). A second rabbit produced a phospho-specific antibody for pSmad1^{GSK3} Ser210 active at dilutions of 1:30,000 after affinity depletion with phospho-Ser214 peptide and positive purification with phospho-Ser210 peptide (antibody A). An additional anti-pSmad1^{GSK3} Ser210 (antibody B), derived with peptide PHSPTSS[PO_3]DPGSPFQ as antigen, detected overexpressed hSmad1-wt but not the phosphorylation-resistant mutant S210A (Figure 1M). Immunoblots of nonradioactive biochemical reactions confirmed that Ser214 in recombinant Smad1 protein was indeed phosphorylated by Erk/MAPK and that the phosphorylation of Ser210 by GSK3 was strongly dependent on prephosphorylation by MAPK and underscored the phospho-specificity of our antibodies (see Figure 1N, lanes 2–4). We conclude that Smad1 is phosphorylated by GSK3 in vitro in a MAPK-dependent fashion.

GSK3 phosphorylations were required for the polyubiquitinylation of Smad1 (Figure 2A). The Smad ubiquitination regulatory factor 1 (Smurf1) E3 ubiquitin ligase binds to a PPXY sequence (Zhu et al., 1999) located near the Smad1 linker MAPK phosphorylation sites (Figure 1A).

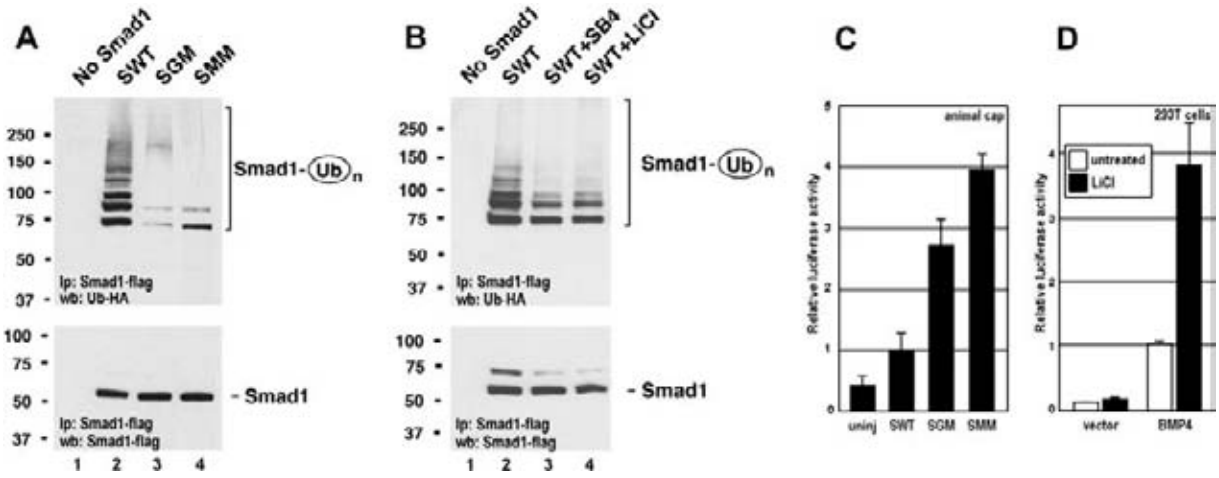

Figure 2. GSK3 and MAPK Phosphorylation Sites Regulate Polyubiquitinylation of Smad1 and Its Transcriptional Activity

(A) Polyubiquitinylation of Smad1 requires GSK3 and MAPK phosphorylation sites. Cells were cotransfected with Smad1-flag, Smurf1, and Ubiquitin-HA.

(B) GSK3 inhibitors decrease polyubiquitinylation of human Smad1. SB415286 (SB4, Biomol) was used at 40 μM, and LiCl at 30 mM, for 24 hr.

(C) *SGM* and *SMM* are more active than *SWT* mRNA in a BRE-luciferase transcriptional reporter assay in ectodermal *Xenopus* explants.

(D) The GSK3 inhibitor LiCl increases BMP4-induced transcriptional activation of BRE-luciferase in 293T cells 8 hr after cotransfection. Data are represented as mean ± standard deviation, three independent experiments.

We used the assay of Zhu et al. (1999) in 293T cells, in which flag-tagged Smad1-WT or its GSK3 or MAPK mutants were cotransfected with HA-tagged ubiquitin and Smurf1, and Smad1 was immunoprecipitated via its flag-tag. Polyubiquitinylation of GSK3 or MAPK phosphorylation-resistant Smad1 proteins (SGM and SMM) was greatly reduced when compared to their wild-type counterpart (Figure 2A, lanes 2–4). The mono- or diubiquitinylated forms were less affected. In addition, polyubiquitinylation of SWT in 293T cells was inhibited by the GSK3 inhibitors SB415286 or lithium chloride (LiCl) (Figure 2B). We conclude that phosphorylation of Smad1 by GSK3 is essential for its polyubiquitinylation in cultured mammalian cells.

We next tested whether the transcriptional activity of Smad1 was regulated by GSK3 phosphorylations. Experiments were performed in *Xenopus* ectodermal explants, which have physiological endogenous BMP signaling levels sufficient for reporter gene studies (Kuroda et al., 2005). It was found that the phosphorylation-resistant mutants SGM and SMM caused significantly stronger induction (3- to 4-fold) of a BMP reporter (BREx2-Id1-luciferase; Korchynskyi and ten Dijke, 2002) than SWT (Figure 2C). In addition, the effect of the GSK3 inhibitor LiCl on BMP-dependent transcription was tested. Cotransfection of *BMP4* and BREx2-Id1-luciferase DNAs into 293T cells showed that LiCl treatment significantly increased the transcriptional activity of endogenous BMP-Smads (Figure 2D). These results were congruent with the microinjection of *SGM* and *SEVE-GM* mRNAs in *Xenopus* embryos (Figures 1E and 1I) and suggested that GSK3 activity normally represses Smad1 signaling by promoting proteasomal degradation.

GSK3 and MAPKs Regulate the Duration of BMP Signals

We next investigated whether the coupled inhibitory phosphorylations by MAPK and GSK3 regulated the duration of the BMP7 signal in pulse-chase experiments (Figure 3). The intensity of the Smad1 signal is determined by the levels of C-terminal phosphorylation (pSmad1^{Cter}) by BMPR (Feng and Derynck, 2005). The phosphorylations of endogenous Smad were analyzed in L cells, which respond particularly well to BMP in serum-free medium (serum complicates analyses because it contains BMP and FGFs). Note that in these and all subsequent cultured cell experiments, endogenous Smad1 was analyzed. By using this assay, we found that the MAPK and GSK3 phosphorylations were triggered by BMPR activity.

A strong pSmad1^{Cter} signal was elicited at time 0 after a 15 min pulse of 5 nM BMP7 (Figure 3A, compare lanes 1 and 2), which partially decreased after 1 hr and greatly diminished by 2.5 hr (lanes 3–5). Interestingly, pSmad1^{MAPK} antibodies also detected a BMP7-induced band, but with a 0.5 hr delay. The pSmad1^{GSK3} antibody detected BMP-induced phosphorylations 0.5 and 1 hr after treatment, which decreased by 2.5 hr (Figure 3A, lanes 2–5). Total Smad1 protein levels did not change during this period; this is in agreement with observations that only a small fraction of the total Smad1 is phosphorylated at physiological BMP levels, with a large reservoir of inactive Smad1 persisting at most times (e.g., Kuroda et al., 2005). BMP treatment does not increase activity levels of the three main cellular MAPKs (Erk, p38, and JNK) (Kuroda et al., 2005; Sapkota et al., 2007; data not shown). Experiments with chemical inhibitors (U0126 for MEK/Erk, Calbiochem CFPD inhibitor for p38, SP600125 for JNK)

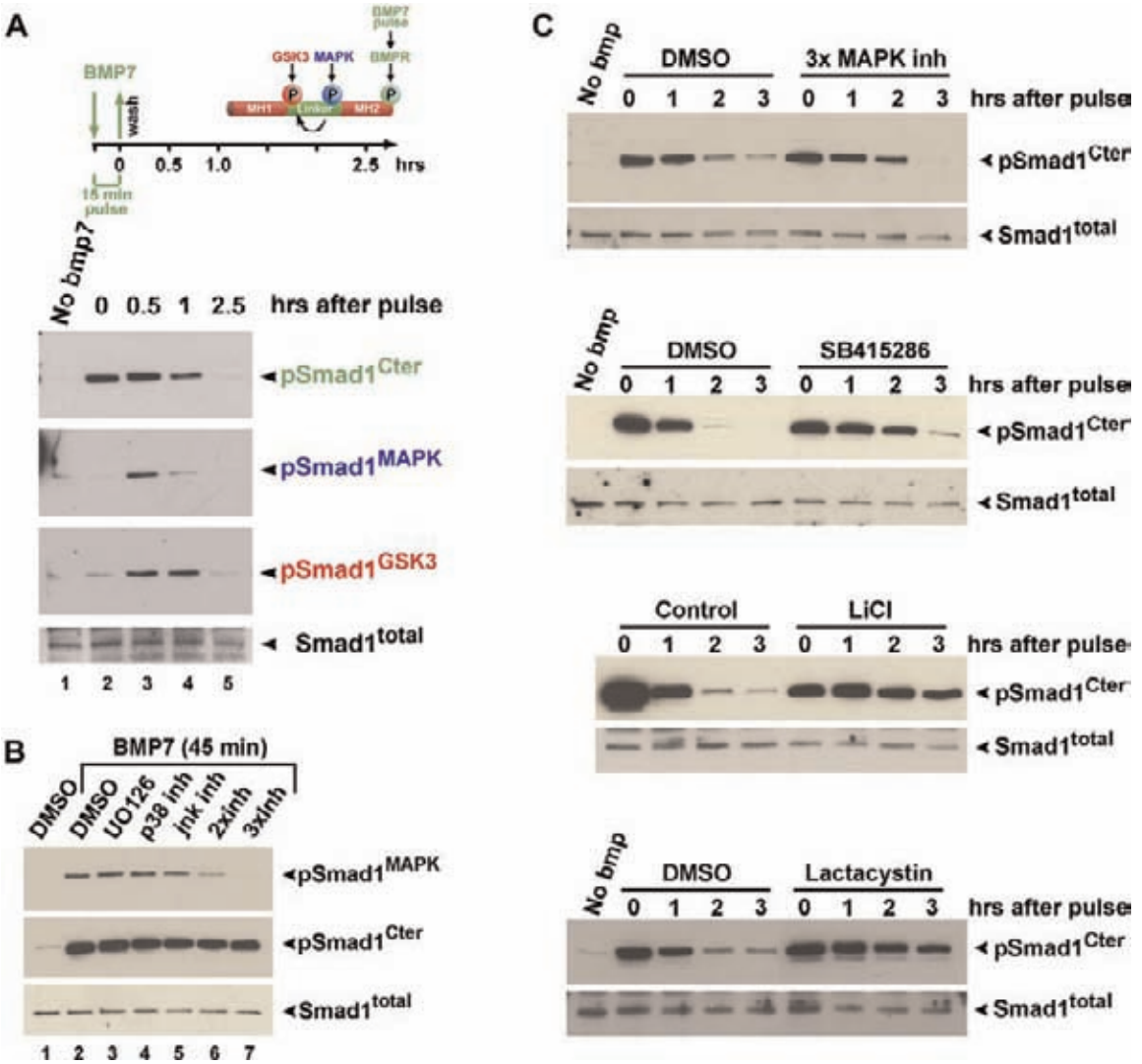

Figure 3. The Duration of the pSmad1^{Cter} Signal Is Regulated by MAPK and GSK3

(A) Sequential phosphorylation of Smad1 by BMPR, MAPK, and GSK3 after a pulse of BMP7.

(B) Induction of pSmad1^{MAPK} by BMP7 is blocked by triple inhibition of MAPKs (lane 7). Inhibitors used were: MEK/Erk (10 μM U0126), p38 (10 μM Calbiochem CFPD p38 inhibitor), and JNK (25 μM SP600125). Lane 6 contained both p38 and JNK inhibitors.

(C) The duration of pSmad1^{Cter} signal is prolonged by inhibition of MAPKs, GSK3 (40 μM SB415286 or 30 mM LiCl), or proteasome activity (50 μM lactacystin).

showed that the Smad1 MAPK phosphorylation triggered by BMP7 results from the combined constitutive activity of these three MAPKs in cultured cells (Figure 3B; Figure S2). We have also observed, with a phosphorylation-resistant C-terminal mutant, that MAPK and GSK3 can phosphorylate Smad1 in a BMPR-independent fashion (data not shown); this activity may help explain why neural induction by Chordin requires an intact MAPK pathway (Pera et al., 2003). Recently, Sapkota et al. (2007) reported that BMP induced MAPK phosphorylation, but suggested the involvement of a different and as yet unknown kinase; however, they did not test a cocktail of the three inhibitors as in Figure 3B (lane 7). We conclude from these pulse-chase experiments that BMP treatment triggers three sequential phosphorylations in Smad1: first by BMPR, second by MAPKs, and third by GSK3.

The sequential nature of these events suggested that they might function in the regulation of the duration of the BMP signal, which would be terminated by the coupled activity of MAPK and GSK3 via degradation in the proteasome. To test this hypothesis, we performed BMP7 pulse-chase experiments in the presence of the MAPK inhibitor cocktail, the GSK3 inhibitors LiCl or SB415286, or the proteasome inhibitor lactacystin. As shown in Figure 3C, all these treatments significantly increased the duration of the pSmad1^{Cter} signal. These results suggest a molecular

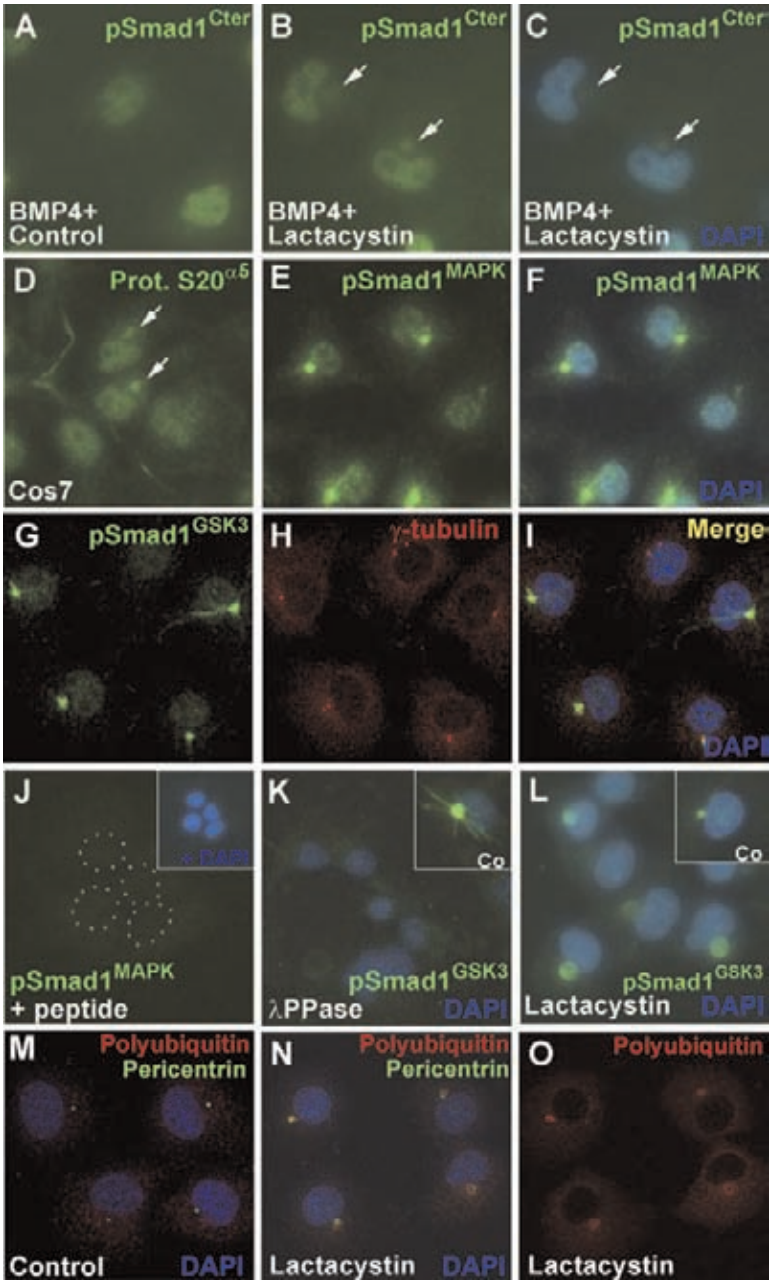

Figure 4. MAPK and GSK3 Phosphorylations Target Smad1 and Total Polyubiquitinated Proteins to the Centrosome in Cos7 Cells

(A–C) pSmad1^{Cter} accumulates in the centrosome (arrows) in response to proteasomal inhibition by lactacystin (24%, n = 323).

(D) The proteasomal subunit S20α5 normally accumulates in the centrosome in Cos7 cells (arrows).

(E and F) Nuclear and centrosomal localization of pSmad1^{MAPK}.

(G–I) pSmad1^{GSK3}-A (green) colocalizes with the centrosome marker γ-Tubulin (red). Note that in (E) through (I), BMP4 was not added, but the medium contained 10% fetal calf serum, which provides growth factors such as BMP and FGF.

(J and K) Specificity of pSmad1^{MAPK} and pSmad1^{GSK3}-A staining: phospho-peptide competition and λ-phosphatase sensitivity.

(L) pSmad1^{GSK3} accumulates in the centrosome 8 hr after lactacystin (50 μM) treatment (a 25-fold increase in volume).

(M–O) Treatment of Cos7 cells with lactacystin induces accumulation of total cellular polyubiquitinylated proteins in the centrosomal region marked by pericentrin in red. In one cell, a ring of pericentrosomal staining is seen.

pathway in which, after phosphorylation by BMPR, the duration of the pSmad1^{Cter} signal is controlled by coupled MAPK and GSK3 phosphorylations and protein degradation in the proteasome.

pSmad1$^{MAPK/GSK3}$ Is Targeted to the Centrosome

Unexpectedly, when the subcellular localization of the various forms of phosphorylated Smad1 in cultured cells was examined, it was found that Smad1 targeted for degradation accumulated in the centrosomal region (Figure 4). The pSmad1^{Cter} antigen accumulates in the nucleus of Cos7 cells after BMP4 treatment in serum-free conditions, but we noted that in cells treated with the proteasome inhibitor lactacystin, pSmad1^{Cter} was also found in a cytoplasmic region (Figures 4B and 4C) that appeared to correspond to the centrosome (when a kidney-shaped nucleus is present, as in Figure 4C, the centrosome is almost invariably located in its concavity; Wilson, 1928). The centrosome, the region of cytoplasm that surrounds the centrioles, is a center for ubiquitin-mediated proteolysis in which the proteasomal machinery becomes concentrated (Badano et al., 2005). We corroborated this by staining Cos7 cells with proteasomal S20α5 subunit antibodies. Proteasomes were present both in nucleus and cytoplasm, but were more concentrated in the centrosome (Figure 4D, arrows).

Phospho-Smad1^{MAPK} was observed both in the nucleus and in a bright centrosome-like body in the cytoplasm (Figures 4E and 4F). The pSmad1^{GSK3} antibody stained the nucleus weakly and the cytoplasm strongly, along microtubule-like filaments that converged on the centrosome, which was unequivocally identified by colocalization with the established centrosomal marker γ-tubulin (Figures 4G–4I). Specificity controls showed that centrosomal phospho-Smad1 staining was eliminated or reduced by competition with the corresponding phosphorylated peptide (Figure 4J), by λ-phosphatase treatment (Figure 4K), and by the MAPK inhibitor cocktail or the GSK3 inhibitor SB415286 (Figure S2). Centrosomal localization was greatly enhanced by treatment of Cos7 cells with the proteasomal inhibitor lactacystin (Figure 4N), supporting the view that Smad1 is degraded by proteasomes located in the centrosome.

Finally, we investigated whether this cellular mechanism represented a wider phenomenon that might apply to other proteins targeted for degradation. An antibody against total polyubiquitin chains stained diffusely both nucleus and cytoplasm (Figure 4M), but after lactacystin treatment, polyubiquitin antigen became clearly concentrated in the pericentrosomal region overlapping, and in some cases surrounding, the Pericentrin centrosomal marker (Figures 4N and 4O). We conclude that the cellular degradation pathway we have identified probably is used by many other proteins marked for destruction in addition to Smad1, because total polyubiquitinylated proteins also became concentrated in centrosomes when proteasome activity was inhibited.

Smad Degradation Is Regulated by Wnt

As shown in the model in Figure 5A, the experiments presented so far suggest that an elaborate cellular regulatory pathway is involved in the termination of BMP signaling. Nuclear C-terminal phosphorylated Smad1 is subjected first to MAPK phosphorylation in the linker region and then to GSK3 phosphorylation, triggering the polyubiquitinylation of Smad1. Once targeted for degradation, Smad1 is transported, probably along microtubules, to the centrosome, where the triply phosphorylated and polyubiquitinylated Smad1 is degraded by proteasomes. A key question, with important implications for the integration of patterning signals, is whether GSK3 phosphorylation of Smad1 is regulated by canonical Wnt signaling.

To investigate this, the effects of treating cultured L cells (in the absence of serum and in the presence of BMP7 and FGF2) with purified Wnt3a protein were examined. The levels of pSmad1^{GSK3} were decreased, but not eliminated, 1 hr after Wnt3a addition, while the levels of pSmad1^{Cter} increased (Figure 5B). The increase in pSmad1^{Cter} was due to stabilization, rather than to secondary induction of BMP ligands, because transfection of *β-catenin* DNA (both in wild-type and stabilized mutant forms) did not significantly affect pSmad1^{Cter} phosphorylation levels in L cells (data not shown). Wnt3a protein also affected Smad1 phosphorylations in human embryonic stem cells (hESCs), causing pSmad1^{GSK3} to decrease moderately and pSmad1^{Cter} to accumulate (Figure 5C). We conclude that the levels of pSmad1^{Cter} are stabilized by Wnt3a treatment, in agreement with the pathway proposed in Figure 5A.

We next investigated whether the activation of Wnt signaling caused a change in the cellular localization of the pSmad1^{GSK3} antigen. A recent study has demonstrated that Wnt signals cause the colocalization of components of the β-Catenin degradation complex, such as GSK3 and Axin, with intracellular membrane vesicles containing the Wnt receptor LRP6 (Bilic et al., 2007). Transfection of *CA-LRP6* DNA (Tamai et al., 2004) into Cos7 cells caused a dispersion of the centrosomal pSmad1^{GSK3} antigen into small cytoplasmic particles when compared to untransfected cells (Figures 5D and 5E). These cytoplasmic puncta most likely correspond to LRP6 signalosomes (Bilic et al., 2007) because they colocalized with endogenous GSK3 protein (Figure 5G). In addition to dispersing the centrosomal material into smaller particles, CA-LRP6 caused the pSmad1^{GSK3} antigen to accumulate in the cell nucleus (Figures 5D–5G). Perhaps transport to the centrosome is required for nuclear export of Smad1 marked for destruction. We conclude that activation of the Wnt pathway triggers a major redistribution of Smad1 forms targeted for degradation within the cell.

We next turned to the *Xenopus* embryo. An old enigma is why overexpression of Wnt antagonists, such as Dkk1, cause dorsalized phenotypes (expanded neural plate at the expense of epidermis) almost indistinguishable to those of embryos microinjected with BMP antagonists, such as Chordin protein (Figures 6A–6C). This suggested the possibility that Wnt inhibitors might regulate BMP signaling at gastrula through the pathway indicated in Figure 6D. This hypothesis was tested by coinjection of *Dkk1* and *Xenopus BMP4* mRNA (Figures 6E–6H). BMP4 overexpression inhibited expression of the forebrain/eye marker *Rx2a*, and *Dkk1* mRNA blocked this inhibition (compare Figures 6G and 6H). Dkk1 is one of the strongest and best characterized inhibitors of canonical Wnt signaling, which functions by removing the LRP6 Wnt coreceptor from the cell surface (Glinka et al., 1998; Niehrs, 2004). Therefore, in principle, Dkk1 should not have inhibited BMP4 signaling.

To explore this in vivo in a Wnt loss-of-function situation, we used a previously characterized *Xenopus laevis* Wnt8 MO (Lee et al., 2006). xWnt8 is the main Wnt expressed posteriorly during gastrulation (Christian and Moon, 1993), and its knockdown causes dorsalization with expansion of brain at the expense of epidermis (marked by *Cytokeratin*) (Figures 6J and 6N). Microinjection of wild-type *Smad1* mRNA had little effect on the xWnt8 depletion phenotype (Figures 6K and 6O), yet injection of the same amount of *SGM* mRNA was able to abrogate the dorsalizing effects of Wnt8 MO (Figures 6L and 6P). This indicates that the GSK3 phosphorylation sites in microinjected Smad1 play a crucial role in the dorsalizing effects caused by Wnt8 depletion. The phosphorylation of Smad1 GSK3

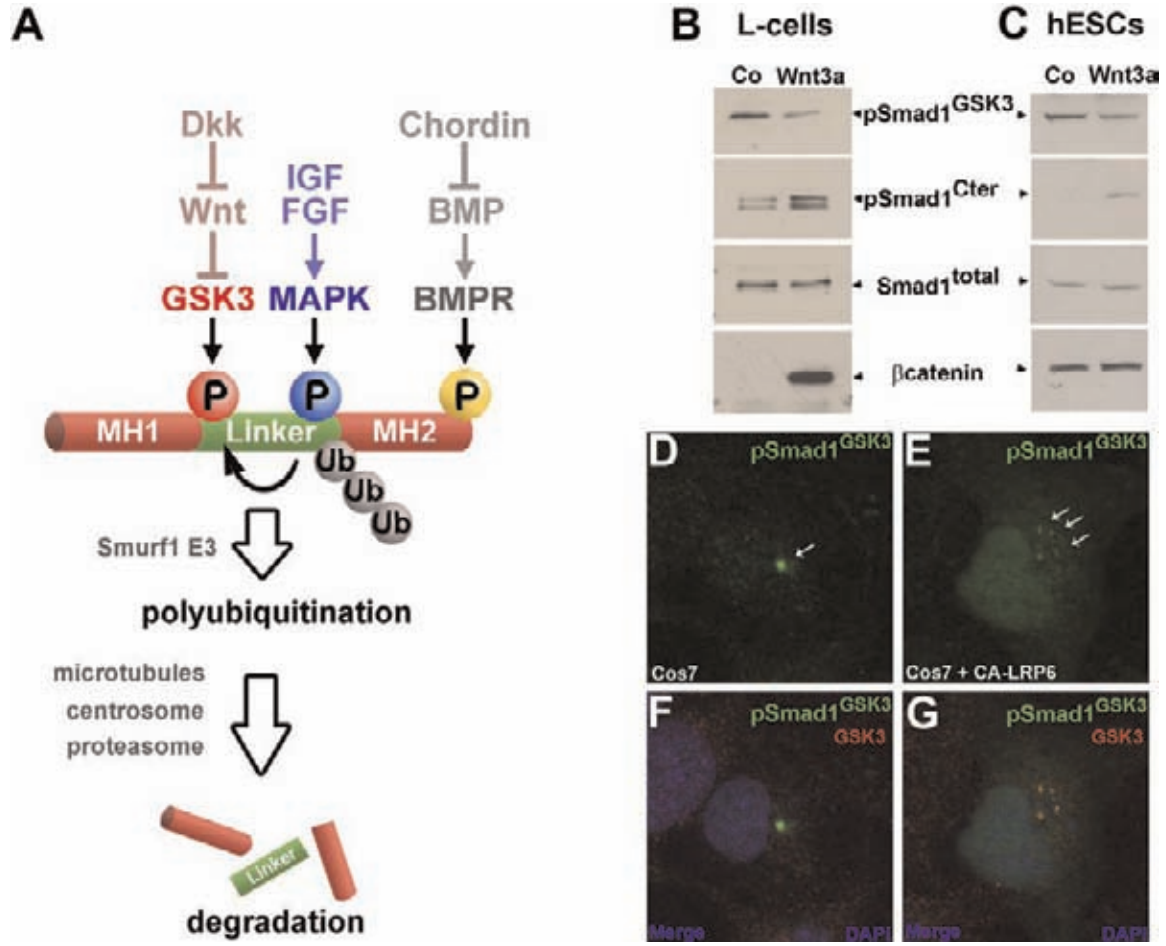

Figure 5. Wnt3a Regulates Smad1 Phosphorylation

(A) Model of biochemical and cellular signaling pathway integration at the level of Smad1 phosphorylations.

(B) Wnt3a protein (300 ng/ml, R&D Systems) inhibits Smad1 phosphorylation by GSK3 and stabilizes pSmad1^{Cter}. L cells cultured in the absence of serum were treated with purified Wnt3a protein for 1 hr; 0.3 nM BMP7 and 40 ng/ml FGF2 were added after 20 min of Wnt treatment.

(C) Wnt3a (300 ng/ml) stabilizes pSmad1^{Cter} and β-Catenin in hESCs after 2 hr.

(D and E) Activation of the Wnt pathway with transfected CA-LRP6 (Tamai et al., 2004) disperses pSmad1^{GSK3} from the centrosome into small cytoplasmic puncta. Note that in CA-LRP6-transfected cells, the levels of pSmad1^{GSK3} in the nucleus are elevated.

(F and G) The cytoplasmic puncta containing pSmad1^{GSK3} most likely correspond to LRP6 signalosomes because they costain with GSK3 antibodies. Transfected cells were identified by cotransfection of CFP, not shown here.

sites requires MAPK priming and, in agreement with this, phosphorylation-resistant *SMM*, but not *SWT* mRNA, also inhibited the effects of Wnt8 MO in the embryo (Figure S3).

Dkk1 overexpression is expected to block all canonical Wnt signaling at gastrula. *Dkk1* mRNA microinjection expanded the neural plate, and overexpressed wild-type Smad1 was ineffective at counteracting this (Figures 6Q–6S), whereas the GSK3 phosphorylation-resistant mutant SGM was able to reverse the enlargement of the neural plate produced by *Dkk1* mRNA (compare Figures 6S and 6T). These epistatic experiments support the hypothesis that the GSK3 phosphorylation sites in Smad1 are critical targets of Dkk1 and Wnt8 signaling during *Xenopus* development.

The Antineural Effects of Wnt/GSK3 Require Smad1 but Not Tcf3

We next investigated the molecular pathway by which Wnt/GSK3 regulates the decision between epidermal and neural cell fates in vivo. In *Xenopus*, it is sufficient to dissociate ectodermal (animal cap) cells to switch from an epidermal to a neural fate (Wilson and Hemmati-Brivanlou, 1995). This default neural differentiation is caused by sustained activation of MAPK/Erk (Kuroda et al., 2005). Ectodermal explants normally differentiate into epidermis, while dissociated animal cap cells form neural tissue (Figure 7A, compare lanes 2 and 3). LiCl, an inhibitor of GSK3, inhibits neural tissue and causes epidermal differentiation (Figure 7A, lanes 3–6).

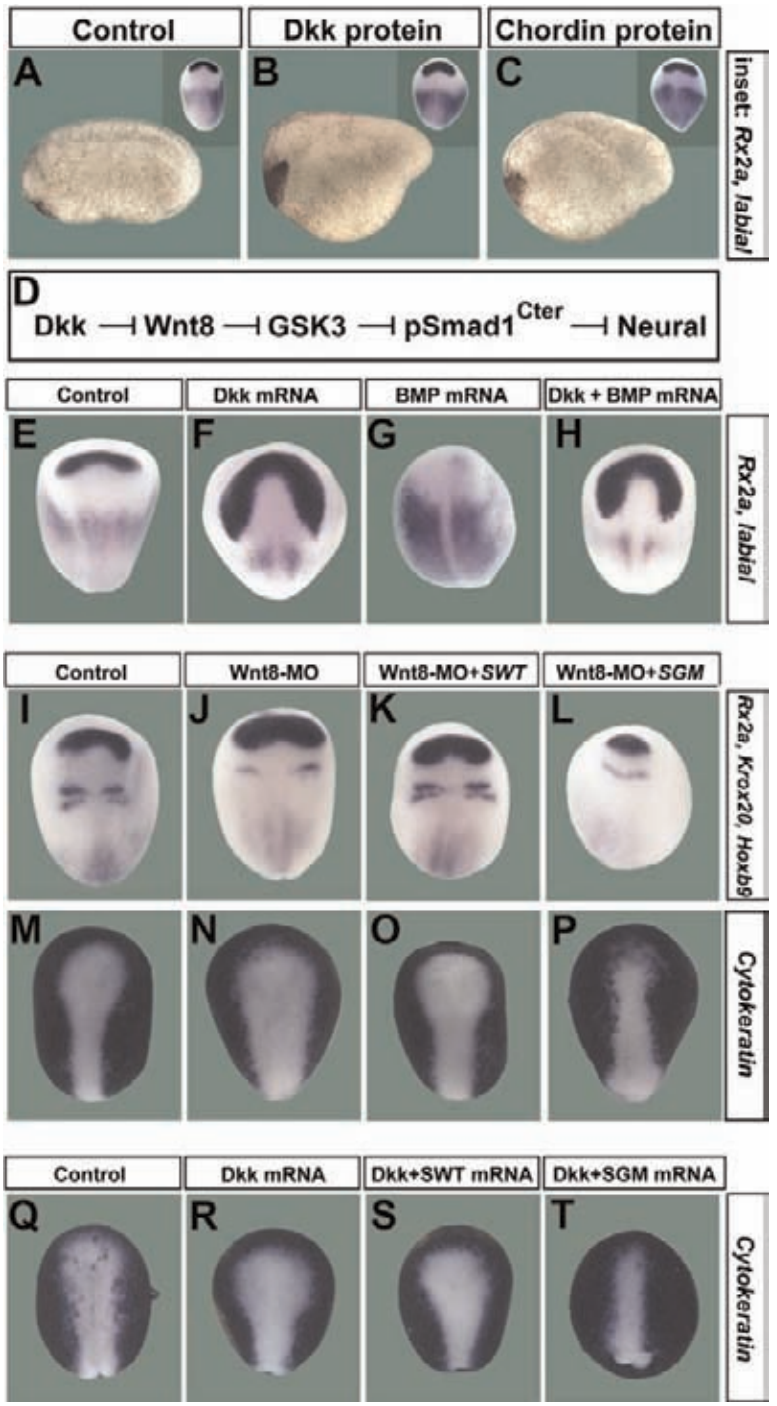

Figure 6. The Dorsalizing Effects of Wnt Inhibition Are Rescued by SGM

(A–C) Dkk1 (n = 28) and Chordin (n = 45) protein (R&D) injections into the blastula cavity (60 nl of 2.5 μM and 0.5 μM, respectively) present considerable phenotypical similarities.

(D) Proposed molecular pathway.

(E–H) *Dkk1* mRNA suppresses the antineural phenotype of BMP4 overexpression (n for each sample was 18, 13, 23, and 18, respectively).

(I–P) Wnt8 MO causes dorsalization, which is blocked by GSK3-resistant *SGM*, but not by *SWT* mRNA (n for each sample was 22, 17, 23, and 26, respectively).

(Q–T) The expansion of the neural plate by *Dkk1* mRNA is rescued by GSK3-resistant *SGM*, but not *SWT* mRNA (n = 30, 22, 21, and 27, respectively).

Microinjection of pCSKA-Wnt8 and pCS2-LRP6 DNA, which are expressed at gastrula stage (Christian and Moon, 1993), induced epidermis 8-fold in dissociated animal cap cells (Figure 7B). Importantly, epidermal induction by Wnt was blocked by coinjection of mRNA encoding a dominant-negative Smad5 mutant mimicking the zebrafish somitabun mutant (mouse DN-Smad5; Beck et al., 2001) that blocks all BMP/Smad1/5/8 signaling (Figure 7B). The epidermal-inducing effect of *Wnt8*/*LRP6* DNA, which was in itself a novel observation, was not caused by an increase of *BMP4* mRNA levels, which did not change significantly when compared to uninjected cells (mean 0.9 ± 0.2 standard deviation) in the same samples. This is in agreement with previous work in *Xenopus* showing that xWnt8 is unable to induce BMP4 (Hoppler and Moon, 1998). In whole embryos, DN-Smad5 eliminated epidermal

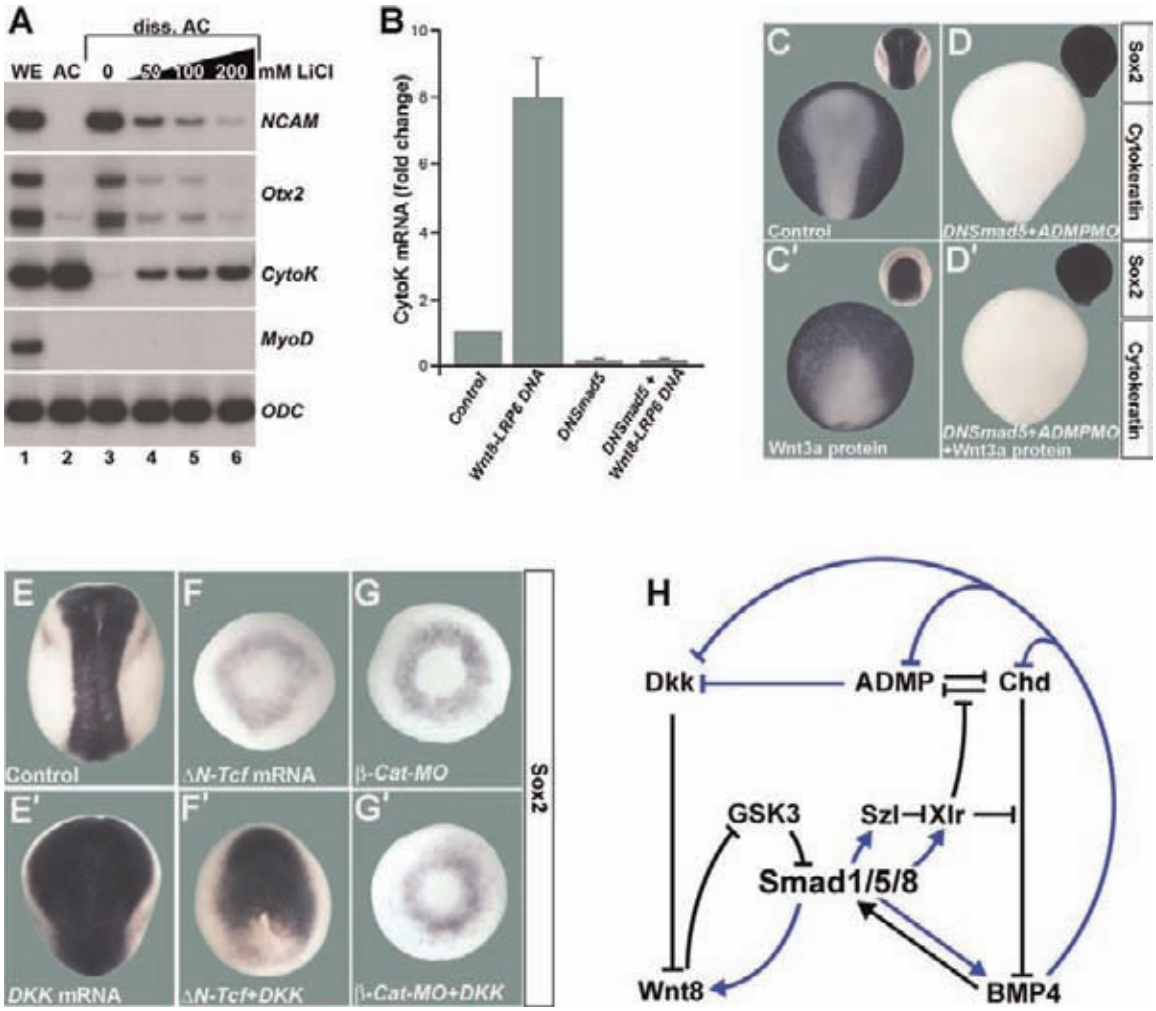

Figure 7. Wnt Signaling Induces Epidermis in a Smad1/5/8- and β-Catenin-Dependent, but Tcf3-Independent, Manner

(A) LiCl induces epidermis (*Cytokeratin*) and inhibits neural differentiation (*NCAM, Otx2*). Radioactive RT-PCR analysis of whole embryos (WE), animal cap (AC) explants, and dissociated animal cap cells at stage 13. *MyoD* indicates lack of mesoderm induction and Ornithine decarboxylase (*ODC*) equal loading.

(B) Quantitative PCR of dissociated animal caps injected with pCSKA-Wnt8 and pCS2-LRP6 DNA. *DN-Smad5* mRNA was coinjected to block Smad1/5/8 activity. *Cytokeratin* mRNA levels at stage 13 were normalized for *ODC* mRNA, and the standard deviation from three independent experiments is indicated.

(C and C′) Wnt3a protein (60 nl of 16 ng/μl) microinjected into the blastula cavity at stage 9 inhibits anterior neural plate and expands epidermis (n = 40 and 42, respectively).

(D and D′) *DN-Smad5* converts the entire ectoderm into neural tissue and is epistatic to Wnt3a protein injection (n = 27 and 35). ADMP MO was coinjected to eliminate all traces of epidermis.

(E and E′) *Dkk1* mRNA expands the neural plate (n = 100 and 53).

(F) *ΔN-Tcf3* mRNA eliminates the neural plate; only a ring of *Sox2* expression in ventral mesoderm remained (90%, n = 30).

(F′) *Dkk1* mRNA rescues neural plate in the presence of *ΔN-Tcf3* in 60% of embryos (n = 70).

(G and G′) The induction of neural plate by *Dkk1* mRNA has a complete requirement for β-Catenin (100%, n = 17 and 55, respectively).

(H) Model in which the BMP (D-V) and Wnt (A-P) patterning pathways are integrated at the level of Smad1/5/8 phosphorylations. Black arrows indicate direct protein-protein interactions and blue arrows transcriptional regulation by Smad1/5/8; all interactions are supported by overexpression or morpholino studies in *Xenopus* (Lee et al., 2006, and data not shown).

differentiation, causing ubiquitous neural differentiation of the entire ectoderm (particularly in the presence of MO for ADMP, a BMP expressed at low Smad1/5/8 signaling levels; Figures 7C and 7D; Reversade and De Robertis, 2005). Microinjection of Wnt3a protein at late blastula expanded the embryonic epidermis but was without effect in a DN-Smad5 background (Figures 7C′ and 7D′). Similarly, GSK3 MO, which expands epidermis and inhibits neural tissue in the whole embryo, was unable to induce epidermis in DN-Smad5 embryos (Figure S4). We conclude

that Wnt/GSK3 signals induce epidermis in *Xenopus* embryos and that this requires an active BMP/Smad1/5/8 pathway.

The canonical Wnt pathway signals by preventing the degradation of β-Catenin, an adaptor protein containing armadillo repeats, which accumulates in the nucleus, binds to the repressor T cell factor 3 (Tcf3), and activates the transcription of Tcf target genes (Molenaar et al., 1996; Logan and Nusse, 2004). This pathway controls patterning in the *Xenopus* embryo during cleavage stages, causing the formation of the early embryonic dorsal axis (Harland, 2000; Heasman, 2006). At the gastrula stage, Wnts (and LiCl) have the opposite effect, promoting the formation of epidermis and ventral tissues (Figure S5B). Because late Wnt signaling appeared to be mediated in part through the regulation of Smad1 activity, we investigated whether the late effects of Wnt signaling in *Xenopus* were dependent on Tcf3 and β-Catenin. *Dkk1* mRNA provides an excellent reagent to explore this because it specifically inhibits all gastrula-stage canonical Wnt signaling. Dkk1 greatly expands the anterior neural plate (Figure 7E′). ΔN-Tcf3 encodes a 31 amino acid deletion lacking the β-Catenin binding site (Molenaar et al., 1996), which once bound to DNA blocks early Wnt signaling, resulting in embryos devoid of neural plate (Figures 7E and 7F). Remarkably, it was found that *Dkk1* mRNA was able to restore neural plate development in 60% of these embryos (Figure 7F′). We also investigated whether the loss of neural plate caused by depletion of β-Catenin could be rescued by Dkk1 and found, to our surprise, a complete requirement for β-Catenin (Figures 7G and 7G′). We conclude from these epistatic experiments that Wnt signaling promotes epidermal development via a Smad-dependent pathway and that Dkk1 promotes neural development in a Tcf-independent, yet β-Catenin-dependent, manner.

DISCUSSION

We investigated the function of the four conserved GSK3 phosphorylation sites in Smad1. During the course of the work, we generated new phospho-specific antibody reagents for pSmad1^{MAPK} and pSmad1^{GSK3} that revealed a cell biological pathway by which the duration of the BMP signal is exquisitely modulated. Three novel observations were made. First, we found that BMP signaling triggers three sequential Smad1 phosphorylations by BMPR, MAPK, and GSK3. Second, we found that the GSK3 and MAPK phosphorylations specifically regulate the duration of the BMP signal. Finally, experiments in cultured mammalian cells and in *Xenopus* embryos indicated that Smad1 phosphorylation by GSK3 serves to integrate the BMP and Wnt signaling pathways.

Sequential Smad1 Phosphorylations

GSK3 phosphorylation required priming by phosphorylated MAPK sites located in the linker region of Smad1. GSK3 phosphorylation-resistant mutations generated hyperactive forms of Smad1, as in the case of MAPK-resistant mutations (Kretzschmar et al., 1997; Pera et al., 2003; Aubin et al., 2004; Sapkota et al., 2007). High-titer phospho-specific antibody reagents for GSK3 (Ser210) and MAPK (Ser214) revealed the biochemical pathway of sequential phosphorylations summarized in Figure 5A. C-terminal phosphorylation by BMPR triggered nuclear translocation (Shi and Massagué, 2003) and was followed about 30 min later by phosphorylation at MAPK sites, presumably in the nucleus. This served as priming for phosphorylation by GSK3. The intracellular site of the GSK3 phosphorylation is not known because GSK3 is found both in nucleus and cytoplasm (Huang et al., 2007). The combination of both MAPK and GSK3 phosphorylations is essential for the polyubiquitinylation of Smad1 by the Smurf1 E3 ubiquitin ligase (Zhu et al., 1999). Recently, an independent study showed that MAPK phosphorylation is essential for Smad1 polyubiquitinylation (Sapkota et al., 2007), a discovery fully confirmed here. One difference between the two studies is that here we report an essential requirement for GSK3 for polyubiquitinylation in vivo, whereas Sapkota et al. (2007) found only a partial impairment in their in vitro studies. The broad theme that emerges from these complementary studies is that linker phosphorylations are required for Smad1 polyubiquitinylation in a negative feedback loop (Sapkota et al., 2007; this work).

Triply phosphorylated Smad1 is polyubiquitinylated, binds to cytoplasmic microtubule-like filaments, and is transported to the centrosome (Figure 4). The centrosome has been described as the proteolytic center of the cell (Badano et al., 2005). Inhibition of the proteolytic activity of proteasomes with lactacystin caused a marked accumulation of phospho-Smad1 destined for degradation specifically in the centrosome. Because, as demonstrated here, total polyubiquitin chains also accumulate in the centrosome after lactacystin treatment, many other proteins targeted for degradation must also use this pathway. The study of Smad1 has led to the identification of an elaborate cellular pathway involved in the degradation of this transcription factor.

The Duration of the Smad1 Signal Is Regulated by a Cellular Proteolytic Pathway

Smad1 is a transcriptional activator that controls the activity of hundreds of downstream target genes (Shi and Massagué, 2003; Feng and Derynck, 2005). During signaling, it is important to control both the intensity and the duration of the signal. The classic example is provided by PC12 cells, in which a transient stimulus of MAPK/Erk by EGF causes cell proliferation, whereas the more sustained activation of Erk caused by NGF induces neuronal differentiation and neurite outgrowth (Marshall, 1995). Whereas the intensity of the Smad1 signal is determined by the dose of BMP, its duration is regulated by the coupled phosphorylations mediated by MAPK and GSK3. Thus, the half-life of phospho-Smad1^{Cter} was prolonged in pulse-chase experiments by inhibiting the three main endogenous MAPKs (Erk, p38, and JNK), GSK3, or proteasomal degradation

(Figure 3). This novel biochemical pathway offers rich possibilities for the differential regulation of target genes by the Smad1 signal.

Integrating the A-P and D-V Axes via Smad1 Phosphorylations

In *Xenopus*, the D-V axis is regulated by a gradient of BMP maximal in the ventral and lowest in the dorsal, and the A-P axis by a gradient of Wnt lowest in the head and highest in the posterior blastopore where xWnt8 is expressed (Niehrs, 2004). When normal patterning is challenged by transplanting a new organizer or cutting the embryo in half, the new pattern is seamlessly integrated (De Robertis, 2006). The model shown in Figure 7H indicates how a self-regulating patterning mechanism may integrate the A-P and D-V axes. This model is based on recent studies on BMP signals and their antagonists (Reversade and De Robertis, 2005; Lee et al., 2006). Smad1/5/8 are presented as key players that can transcriptionally activate ventral genes (BMP4, the protease Xolloid-related, and its inhibitor Sizzled) as well as xWnt8. Previous work has shown that BMP4 is required for the expression of xWnt8, whereas xWnt8 does not affect BMP4 levels in the *Xenopus* gastrula (Hoppler and Moon, 1998). On the dorsal side, BMP signals inhibit the transcription of genes such as ADMP (a dorsal BMP-like molecule), Chordin, and Dkk1. The additional layer of regulation of Smad1/5/8 by MAPKs activated by RTKs such as FGFR, IGFR, and EGFR was not included for simplicity. The key new node of interaction in this modified patterning network is that Wnt8 inhibits the phosphorylation of Smad1 by GSK3, resulting in a longer BMP signal which, in turn, is inhibited by Dkk1. In this view, the D-V axis would be specified by the intensity of the BMP signal and the A-P positional information by its duration.

Our model proposes that Wnt enhances the BMP/Smad1 signal. Such a molecular pathway could have implications for the pathogenesis of hereditary bone diseases. BMPs were isolated as potent inducers of bone morphogenesis, yet recent genetic studies in humans and mice have shown that the Wnt coreceptor LRP5 plays a central role in bone mineralization. Loss-of-function mutations in LRP5 cause osteoporosis and gain-of-function mutations cause osteopetrosis (reviewed in Koay and Brown, 2005). Conversely, heterozygosity of Dkk1, an LRP5/6 inhibitor, causes excessive bone mass formation (Morvan et al., 2006). Like Dkk1, Sclerostin (SOST) is a Wnt antagonist that binds to LRP5/6 and leads to increased bone mass in loss-of-function mutations (Semenov et al., 2005). It would be interesting to determine whether these osteoblast differentiation syndromes are caused by misregulation of the duration of the Smad1/5/8 signal through the Wnt/GSK3 pathway.

The canonical Wnt pathway can inhibit GSK3 activity causing β-Catenin stabilization (Logan and Nusse, 2004). Wnt3a protein moderately decreased $pSmad1^{GSK3}$ levels while increasing the activated $pSmad1^{Cter}$ form (Figure 5). In cytological analyses, activation of the Wnt pathway by a CA-LRP6 caused a striking change. The $pSmad1^{GSK3}$ antigen lost its centrosomal localization and was detected in intracellular puncta corresponding to the recently discovered LRP6 signalosomes that contain GSK3 and other components of the Wnt-regulated protein degradation complex (Bilic et al., 2007). In addition, $pSmad1^{GSK3}$ levels in the nucleus increased in cells transfected with CA-LRP6. This redistribution from the centrosome into putative signalosomes explains the residual levels of $pSmad1^{GSK3}$ found in Wnt-treated cells. Relocation of GSK3 away from the cellular proteolytic center located in the centrosome may disrupt the flow of Smad1 targeted for degradation and suffice to explain the stabilization of $pSmad1^{Cter}$ caused by Wnt3a protein, as well as the increase of $pSmad1^{GSK3}$ levels in the nucleus. Perhaps other features of the canonical Wnt/GSK3 pathway, such as the stabilization of β-Catenin, are mediated by the relocation of Wnt-regulated protein destruction complexes away from the centrosomal proteasomes (Bilic et al., 2007).

The new Wnt signaling branch identified here requires Smad1 and is independent of Tcf3, yet requires β-Catenin (Figure 7). This requirement suggests that both β-Catenin and Smad1 might be degraded by a common Wnt-regulated destruction complex containing GSK3, Axin, and other components (Logan and Nusse, 2004). In this regard, we note that β-Catenin has a primary structure related to armadillo domain adaptor proteins and may help carry Smad1, and perhaps other proteins, to their destruction. A direct interaction between Smad4 and β-Catenin has been reported (Nishita et al., 2000). In addition, β-Catenin binds to the microtubular motor Dynein (Ligon et al., 2001) and β-Catenin can localize to microtubules (Huang et al., 2007). An attractive working hypothesis is that the destruction of β-Catenin could serve to drive the flow of Smad1 targeted for degradation to the centrosome. In *Drosophila*, work currently under completion supports the view that Wingless can stabilize the Mad transcription factor (E.E., L.C.F., J. Clemens, and E.M. De R., unpublished data). With 1500 transcription factors in the human genome, one might predict that in future the degradation of other proteins may also be found to be stabilized by Wnt/GSK3 signaling.

EXPERIMENTAL PROCEDURES

Mammalian Cell Culture Experiments

Mouse L fibroblasts, Cos7, and HEK293T cells were cultured in DMEM supplemented with 10% fetal bovine serum (GIBCO) and cultured at 37°C in 5% CO_2. For pulse-chase experiments, L cells were incubated in serum-free medium (1/3 Iscove's, 2/3 F12 DMEM, GIBCO) for 4 hr, and 5 nM BMP7 added for 15 min. Chemical inhibitors were added 1 hr prior to the BMP7 pulse. Wnt3a protein (R&D Systems) was added at 300 ng/ml in the absence of serum. FGF-2 (Invitrogen) and BMP4 (R&D Systems) were added at 40 ng/ml and 0.3 nM, respectively. CA-LRP6 (LRP6-ΔN, Tamai et al., 2004) was transfected into Cos7 cells with Fugene HD (Roche). We note that the pericentrosomal region is best visualized in sparse cell cultures well below confluence at the G1 phase. Ubiquitination assays were performed as described by Zhu et al. (1999).

Western Blots and Immunostainings

Western blots of endogenous proteins were as described (Kuroda et al., 2005), with polyclonal rabbit antibodies against pSmad1^{MAPK} (1:30,000), pSmad1^{GSK3}-A (1:15,000), pSmad1^{Cter} (1:1000; Cell Signaling), and total Smad1 (1:1000; Zymed). β-catenin antibody (Sigma, 1:8000), GSK3β antibody (BD Transduction Labs, 1:1000), anti-His antibody (Santa Cruz, 1:1000), and anti-flag-HRP conjugate (Sigma, 1:1500) were also utilized. Synthetic peptide was used to immunize two rabbits (Covance). A second pSmad1^{GSK3} antibody phosphorylated at site 210 (designated B) that works on Western blots was generated. For cell immunostaining, primary antibodies were used as follows: pSmad1^{MAPK} (1:2500), pSmad1^{GSK3} (1:1500), total polyubiquitin (1:500, Biomol), proteasome 20Sα5 subunit (1:200, Abcam), γ-Tubulin (1:500, Sigma), and Pericentrin (1:1000, Abcam). For additional immunostaining methods, see Supplemental Experimental Procedures.

In Vitro Phosphorylations

His-tagged linker region (residues 146–264) of Smad1 was cloned in the periplasmic expression vector pET26b, expressed in *E. coli* BL21 cells, and purified with His Bind Resin (Novagen). The priming reaction was performed for 40 min at 30°C in kinase buffer (8 mM MOPS [pH 7.3], 0.2 mM EDTA, 10 mM $MgCaH_3PO_4$, and 20 mM $MgCl_2$) containing 1 mM cold ATP and 5 U/μl recombinant p42/Erk2 (New England Biolabs). After heat inactivation of Erk (65°C for 20 min), a second reaction containing [γ-^{32}P]ATP (Amersham) and recombinant GSK3β (Upstate) was performed for 1 hr at 30°C.

Xenopus Microinjections

All microinjections were four times marginal (or in the animal pole for ectodermal explants) at the 4-cell stage. Amounts injected per blastomere were as follows: Xwnt8 MO (10 ng; Lee et al., 2006), ADMP-MO (8.5 ng), β-catenin-MO (11 ng at 2-cell stage), pCSKA-Wnt8 DNA (30 pg, Christian and Moon, 1993), pCS2-LRP6 DNA (10 pg, Tamai et al., 2004), *ΔN-xTCF3* mRNA (200 pg, Molenaar et al., 1996), *DN-Smad5* mRNA (100 pg, Beck et al., 2001), *Dkk1* mRNA (50 pg per embryo, Glinka et al., 1998), *xBMP4* mRNA (50 pg), *hSmad1* mRNA or its linker mutants (375 ng), and the constitutively active phospho-mimetic hSmad1 SEVE or its linker mutants (200 pg). Luciferase assays were as described in Kuroda et al. (2005). For quantitative PCR, RNA was isolated with Absolutely RNA preparation kit (Stratagene), DNase treated, and reverse transcribed with random primers. SYBR Green real-time quantitative PCR was performed in a MX3000 Cycler (Stratagene). Methods for mRNA synthesis, whole-mount in situ hybridizations, and PCR primers are available at http://www.hhmi.ucla.edu/derobertis/index.html.

Supplemental Data

Five figures and Experimental Procedures are available at http://www.cell.com/cgi/content/full/131/5/980/DC1/.

ACKNOWLEDGMENTS

We thank Drs. G. Thomsen, J. Massagué, D. Bohmann, X. He, R. Moon, J. Slack, H. Clevers, P. ten Dijke, and C. Niehrs for reagents, Y. Sun for advice, and members of our laboratory for comments on the manuscript. This work was supported by the NIH (HD21502-21). C.H. was a recipient of a Heart & Stroke Foundation of Canada Fellowship. E.M. De R. is an investigator of the Howard Hughes Medical Institute.

Received: March 2, 2007
Revised: July 29, 2007
Accepted: September 13, 2007
Published online: November 30, 2007

REFERENCES

Aubert, J., Dunstan, H., Chambers, I., and Smith, A. (2002). Functional gene screening in embryonic stem cells implicates Wnt antagonism in neural differentiation. Nat. Biotechnol. *20*, 1240–1245.

Aubin, J., Davy, A., and Soriano, P. (2004). *In vivo* convergence of BMP and MAPK signaling pathways: impact of differential Smad1 phosphorylation on development and homeostasis. Genes Dev. *18*, 1482–1494.

Badano, J.L., Teslovich, T.M., and Katsanis, N. (2005). The centrosome in human genetic disease. Nat. Rev. Genet. *6*, 194–205.

Beck, C.W., Whitman, M., and Slack, J.M. (2001). The role of BMP signaling in the outgrowth of the *Xenopus* tail bud. Dev. Biol. *238*, 303–314.

Bilic, J., Huang, Y.L., Davidson, G., Zimmermann, T., Cruciat, C.M., Bienz, M., and Niehrs, C. (2007). Wnt induces LRP6 signalosomes and promotes Dishevelled-dependent LRP6 phosphorylation. Science *316*, 1619–1622.

Christian, J.L., and Moon, R.T. (1993). Interactions between *Xwnt-8* and Spemann organizer signaling pathways generate dorsoventral pattern in the embryonic mesoderm of *Xenopus*. Genes Dev. *7*, 13–28.

Cohen, P., and Frame, S. (2001). The renaissance of GSK3. Nat. Rev. Mol. Cell Biol. *2*, 769–776.

De Robertis, E.M. (2006). Spemann's organizer and self-regulation in amphibian embryos. Nat. Rev. Mol. Cell Biol. *7*, 296–302.

De Robertis, E.M., and Kuroda, H. (2004). Dorsal-ventral patterning and neural induction in *Xenopus* embryos. Annu. Rev. Cell Dev. Biol. *20*, 285–308.

Feng, X.H., and Derynck, R. (2005). Specificity and versatility in TGF-β signaling through Smads. Annu. Rev. Cell Dev. Biol. *21*, 659–693.

Glinka, A., Wu, W., Delius, H., Monaghan, A.P., Blumenstock, C., and Niehrs, C. (1998). Dickkopf-1 is a member of a new family of secreted proteins and functions in head induction. Nature *391*, 357–362.

Harland, R. (2000). Neural induction. Curr. Opin. Genet. Dev. *10*, 357–362.

Heasman, J. (2006). Patterning the early *Xenopus* embryo. Development *133*, 1205–1217.

Hoppler, S., and Moon, R.T. (1998). *BMP-2/-4* and *Wnt-8* cooperatively pattern the *Xenopus* mesoderm. Mech. Dev. *71*, 119–129.

Huang, P., Senga, T., and Hamaguchi, M. (2007). A novel role of phospho-β-catenin in microtubule regrowth at centrosome. Oncogene *26*, 4357–4371.

Koay, M.A., and Brown, M.A. (2005). Genetic disorders of the LRP5-Wnt signalling pathway affecting the skeleton. Trends Mol. Med. *11*, 129–137.

Korchynskyi, O., and ten Dijke, P. (2002). Identification and functional characterization of distinct critically important bone morphogenetic protein-specific response elements in the Id1 promoter. J. Biol. Chem. *277*, 4883–4891.

Kretzschmar, M., Doody, J., and Massagué, J. (1997). Opposing BMP and EGF signaling pathways converge on the TGF-β family mediator Smad1. Nature *389*, 618–622.

Kuroda, H., Fuentealba, L., Ikeda, A., Reversade, B., and De Robertis, E.M. (2005). Default neural induction: neuralization of dissociated *Xenopus* cells is mediated by Ras/MAPK activation. Genes Dev. *19*, 1022–1027.

Lee, H.X., Ambrosio, A.L., Reversade, B., and De Robertis, E.M. (2006). Embryonic dorsal-ventral signaling: secreted frizzled-related proteins as inhibitors of tolloid proteinases. Cell *124*, 147–159.

Ligon, L.A., Karki, S., Tokito, M., and Holzbaur, E.L. (2001). Dynein binds to β-Catenin and may tether microtubules at adherens junctions. Nat. Cell Biol. *3*, 913–917.

Liu, C., Li, Y., Semenov, M., Han, C., Baeg, G.-H., Tan, Y., Zhang, Z., Lin, X., and He, X. (2002). Control of β-Catenin phosphorylation/degradation by a dual-kinase mechanism. Cell *108*, 837–847.

Logan, C.Y., and Nusse, R. (2004). The Wnt signaling pathway in development and disease. Annu. Rev. Cell Dev. Biol. *20*, 781–810.

Marcus, E.A., Kintner, C., and Harris, W. (1998). The role of GSK3β in regulating neuronal differentiation in *Xenopus laevis*. Mol. Cell. Neurosci. *12*, 269–280.

Marshall, C.J. (1995). Specificity of receptor tyrosine kinase signaling: treatment versus sustained extracellular signal regulated kinase activation. Cell *80*, 179–185.

Molenaar, M., van de Wetering, M., Oosterwegel, M., Peterson-Maduro, J., Godsave, S., Korinek, V., Roose, J., Destrée, O., and Clevers, H. (1996). XTcf-3 transcription factor mediates beta-catenin-induced axis formation in *Xenopus* embryos. Cell *86*, 391–399.

Morvan, F., Boulukos, K., Clément-Lacroix, P., Ramon Roman, S., Suc-Royer, I., Vayssière, B., Ammann, P., Martin, P., Pinho, S., Pognonec, P., et al. (2006). Deletion of a single allele of the *Dkk1* gene leads to an increase in bone formation and bone mass. J. Bone Miner. Res. *21*, 934–945.

Niehrs, C. (2004). Regionally specific induction by the Spemann-Mangold organizer. Nat. Rev. Genet. *6*, 425–434.

Nishita, M., Hashimoto, S.O., Ogata, S., Laurent, M.N., Ueno, N., Shibuya, H., and Cho, K.W. (2000). Interaction between Wnt and TGF-β signalling pathways during formation of Spemann's Organizer. Nature *403*, 781–785.

Pera, E.M., Ikeda, A., Eivers, E., and De Robertis, E.M. (2003). Integration of IGF, FGF, and anti-BMP signals via Smad1 phosphorylation in neural induction. Genes Dev. *17*, 3023–3028.

Reversade, B., and De Robertis, E.M. (2005). Regulation of ADMP and BMP2/4/7 at opposite embryonic poles generates a self-regulating morphogenetic field. Cell *123*, 1147–1160.

Sapkota, G., Alarcon, C., Spagnoli, F.M., Brivanlou, A.H., and Massagué, J. (2007). Balancing BMP signaling through integrated outputs into the Smad linker. Mol. Cell *25*, 441–454.

Semenov, M., Tamai, K., and He, X. (2005). SOST is a ligand for LRP5/LRP6 and a Wnt signaling inhibitor. J. Biol. Chem. *280*, 26770–26775.

Shi, Y., and Massagué, J. (2003). Mechanisms of TGF-beta signaling from cell membrane to the nucleus. Cell *113*, 685–700.

Stern, C.D. (2005). Neural induction: old problem, new findings, yet more questions. Development *132*, 2007–2021.

Tamai, K., Zeng, X., Liu, C., Zhang, X., Harada, Y., Chang, Z., and He, X. (2004). A mechanism for Wnt coreceptor activation. Mol. Cell *13*, 149–156.

Wilson, E. (1928). The Cell in Development and Heredity (New York: The MacMillan Company).

Wilson, S., and Edlund, T. (2001). Neural induction: toward a unifying mechanism. Nat. Neurosci. *4*, 1161–1168.

Wilson, P.A., and Hemmati-Brivanlou, A. (1995). Induction of epidermis and inhibition of neural fate by BMP4. Nature *376*, 331–333.

Zhu, H., Kavsak, P., Abdollah, S., Wrana, J.L., and Thomsen, G.H. (1999). A SMAD ubiquitin ligase targets the BMP pathway and affects embryonic pattern formation. Nature *400*, 687–693.

Supplemental Data

Integrating Patterning Signals:

Wnt/GSK3 Regulates the Duration

of the BMP/Smad1 Signal

Luis C. Fuentealba, Edward Eivers, Atsushi Ikeda, Cecilia Hurtado, Hiroki Kuroda, Edgar M. Pera, and Edward M. De Robertis

Supplemental Experimental Procedures

Additional Cell Staining Methods

For immunostainings, Cos7 were grown on Lab-tek II 2-well chamber slides (Nalge Nunc). Cells were fixed in fresh paraformaldehyde (4% in PBS for 15 min), followed by permeabilization with 0.2% Triton X100 in PBS for 10 min. The antibodies also worked well after fixation in pure methanol at -20°C for 6 min followed by PBS washes and blocking solution (5% goat serum and 0.5% BSA in PBS). Primary antibodies were diluted in 1:5 blocking solution:PBS and 500 μl applied to each slide chamber, incubated overnight at 4°C, washed 2x in PBS, followed by 2x blocking solution washes, before applying secondary Alexa 488-conjugated anti-rabbit (1:1000; Molecular Probes) or Cy3-conjugated anti-mouse (1:500; Jackson Labs) for 1 hr at room temperature. After washing 3x in PBS, the slides chambers were removed, and the glass slides mounted on DAPI-containing Vectashield (Vector).

Supplemental Reference

Onai, T., Sasai, N., Matsui, M., and Sasai, Y. (2004). Xenopus XsalF: Anterior neuroectodermal specification by attenuating cellular responsiveness to Wnt signaling. Dev. Cell *7*, 95-102.

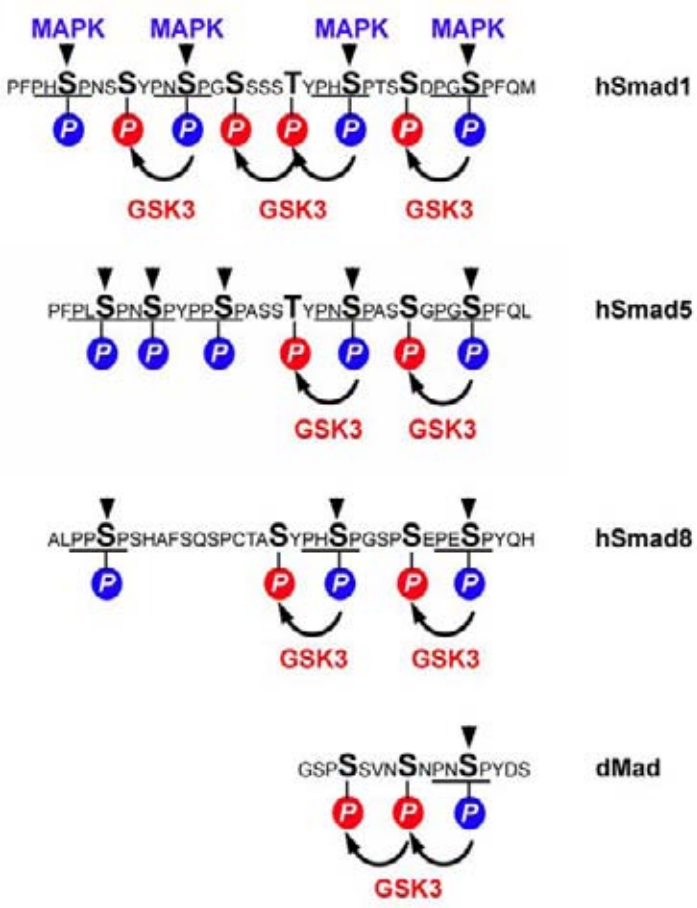

Figure S1. **Conserved Potential GSK3 Phosphorylation Sites**

GSK3 sites (in red) are present in Ser/Thr residues located four amino acids upstream of the MAPK sites (PXSP, in blue) in the linker (middle) region of human Smad1/5/8 as well as in their *Drosophila* homologue Mad. The GSK3 sites are conserved throughout vertebrate BMP-Smads, as well as in Smad4 (not shown). Note that *Drososphila* presents a particularly favorable situation for experimental analysis, since it has a single Mad transcription factor, instead of three as in vertebrates, with a single MAPK site and only two GSK3 phosphorylation sites. Studies in *Drososphila* Mad are currently being pursued (E.E., L.C.F., J. Clemens and E.M.D.R.).

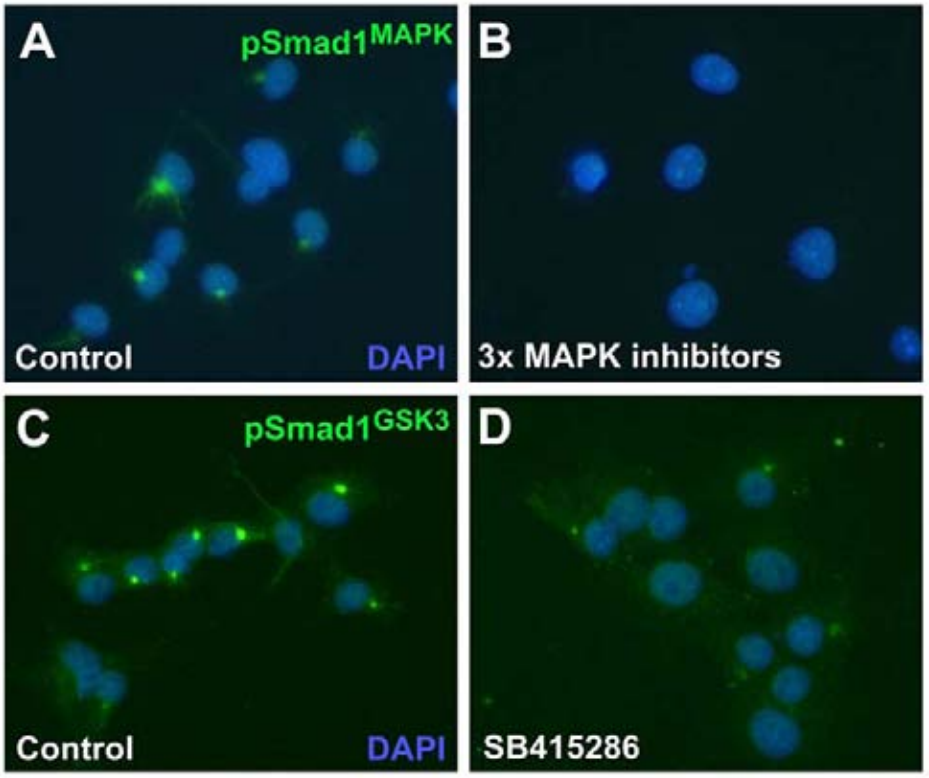

Figure S2. Phospho-Smad1^{MAPK} and Phospho-Smad1^{GSK3} Antigen Localization in the Centrosome Requires MAPK and GSK3 Activities

(A) pSmad1^{MAPK} antigen immunostains a single bright spot corresponding to the centrosome in Cos7 cells. Note that microtubule-like fibers converge on the centrosome and are also stained. Centrosomal staining is strongest in sparse, non-confluent cell cultures. DAPI stains the nuclear DNA in blue.
(B) Antibody staining of pSmad1^{MAPK} was blocked by triple inhibition of cellular MAPK enzymes. A cocktail of three inhibitors targeting: 1) MEK, the MAPKK that activates Erk (10 μM UO126), 2) p38 (10 μM CFPD p38 inhibitor) and 3) JNK (25 μM SP600125) when added to Cos7 cells for 2 hours. All inhibitors were obtained from Calbiochem. This experiment demonstrates that the pSmad1^{MAPK} antigen centrosomal localization requires MAPK activity.
(C-D) Centrosomal localization of pSmad1^{GSK3} is inhibited by treatment with the chemical GSK3 inhibitor SB415286 (BIOMOL) at 40 μM for 2 hours.

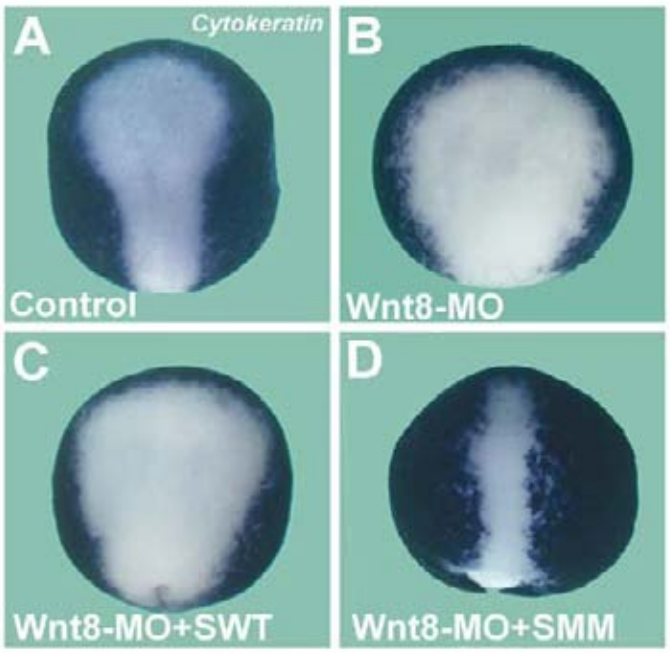

Figure S3. Phosphorylation-Resistant Mutation of the MAPK Sites in Smad1 Are Able to Counteract the Dorsalizing Effects of Wnt8 Depletion in *Xenopus*

(A) Cytokeratin probe delineates the neural plate at stage 13 (n= 30).
(B) xWnt8 MO (Lee et al., 2006) expands the neural plate at the expense of epidermis (n= 24).
(C) Smad1-WT mRNA is unable to inhibit the expansion of the neural plate caused by xWnt8 depletion (100%, n=16).
(D) Co-injection of Smad1-MM mutated at the four MAPK sites is able to overcome the neural plate expansion caused xWnt8 depletion (100%, n= 40). This result shows that the inactivation of the sites that prime GSK3 phosphorylations in Smad1 produce identical phenotypes to those caused by Smad1-GM mRNA (Figure 6P).

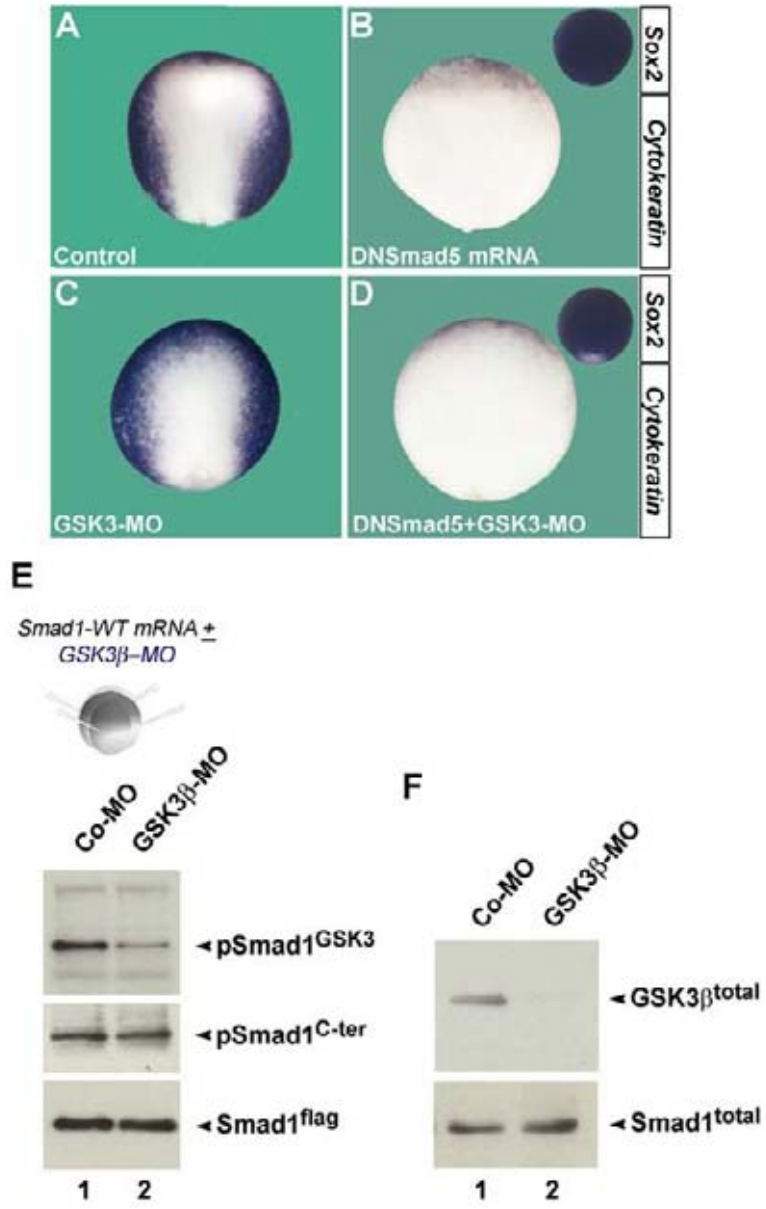

Figure S4. GSK3β MO Reduces the Neural Plate and Expands Epidermis in Wild-Type Embryos but It Is without Effect in Embryos Dorsalized by Dominant-Negative-Smad5; GSK3β Phosphorylates Smad1 In Vivo

(A, B) DN-Smad5 prevents epidermal differentiation (n=18) except for some very weak *Cytokeratin* staining (which can be eliminated by coinjection of ADMP MO as in Figure 7D). The entire ectoderm stains positive for the neural marker *Sox2* (100%, n=20).

(C) Microinjection of 8.5 ng of GSK3β MO reduces the anterior neural plate and correspondingly expands the epidermal territory (82%, n=11), as previously reported by Onai et al. (2004).

(D) DN-Smad5 is epistatic over GSK3β MO (100%, n=18). The entire ectoderm remains neural.

(E) GSK3β MO specifically inhibits the phosphorylation of Ser-210 in microinjected flag-Smad1-WT in stage 10 *Xenopus* embryos. This experiment demonstrates that Smad1 is indeed phosphorylated by GSK3β in vivo.

(F) GSK3β MO inhibits the translation of endogenous *Xenopus* GSK3β protein (assayed with anti-GSK3β antibody from BD Transduction Laboratories at 1:1000 dilution), but not that of total endogenous Smad1 protein which serves as a loading control. Embryos were injected with GSK3β MO at 4-cell and cultured until stage 12 (late gastrula).

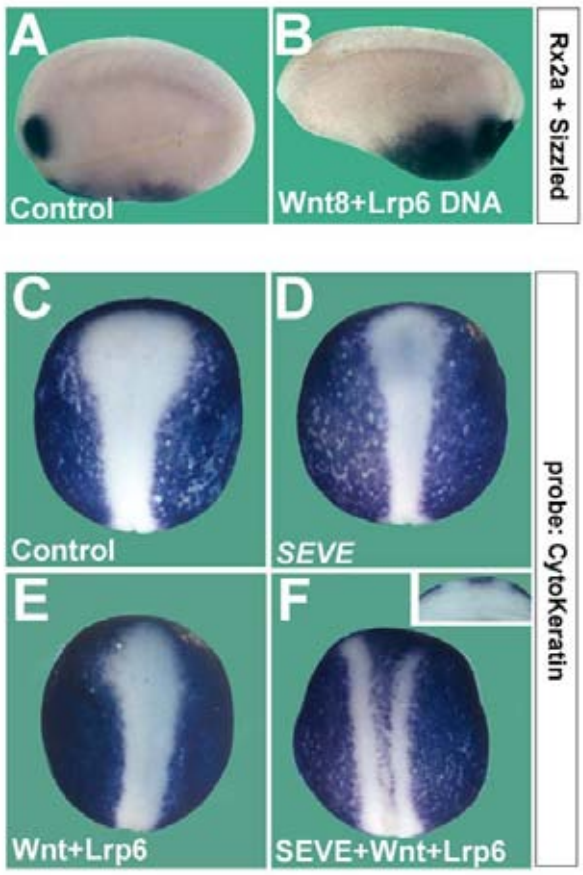

Figure S5. Coinjection of Wnt8 and LRP6 DNA Causes Ventralization of the *Xenopus* Embryo and Synergizes with CA-Smad1-EVE to Induce Epidermis in the Floor Plate Region

(A,B) Microinjection of 30 pg pCSKA-Wnt8 (Christian and Moon, 1993) together with 10 pg of pCS2-LRP6 (Tamai et al., 2004) DNA strongly ventralized the *Xenopus* embryo (95%, n=19). Note that expression of the forebrain/eye marker *Rx2a* is decreased or absent, while the ventral center gene *Sizzled* is increased. This phenotype is typical of *Xenopus* embryos with increased BMP signaling levels (as seen, for example, in Chordin or Sizzled depleted embryos, Lee et al., 2006). Preliminary titrations showed that the response to Wnt8 DNA expressed at the gastrula stage was stronger when its receptor LRP6 is also co-expressed (data not shown).

(C-E) The size of the neural plate, outlined by the epidermal marker *cytokeratin*, is decreased by injection of the constitutively active Smad1 phospho-mimetic mutant Smad1^{EVE} (SEVE) mRNA or Wnt8 plus LRP6 DNA (n=10, 5 and 10 respectively).

(F) When SEVE, Wnt8 and LRP6 mRNAs were coinjected, the embryos were strongly ventralized and the floor plate expressed ectopic cytokeratin in the neural midline (n=12, of which 50% had ectopic epidermis in the midline of the neural plate, see inset). This result provides strong evidence that Wnt8 signals through Smad1 to induce ectopic epidermis in the neural plate midline. This is because Wnt/LRP6 does not induce epidermis in the floor plate in the absence of injected BMP-independent activated Smad1 (SEVE). The only other case in which we have observed this very unusual phenotype of epidermis in the floor plate was in embryos injected with SEVE mRNA mutated either in the MAPK or GSK3 sites (data not shown).